Journal of Environment Sciences (2024), **Volume X**, 19-33
https://doi.org/10.3126/jes.v10i1.66914

Potential Sources and Seasonal Transport Pathways of Organic and Elemental Carbon in the Lesser Himalayan Zone of Central Nepal

Kundan Chaudhary[1*], Sanjay Nath Khanal[1, 2] and Kundan Lal Shrestha[1]
[1] Department of Environmental Science and Engineering, Kathmandu University, Dhulikhel, Nepal
[2] School of Environmental Science and Management, Pokhara University, Kathmandu, Nepal
[*]Correspondence: kundanchaudharynp@gmail.com

Abstract

Carbonaceous aerosols consist of a bulky but highly variable mass of atmospheric aerosols, mostly comprised of Organic Carbon (OC) and Elemental Carbon (EC). OC is emitted directly into the atmosphere or formed secondarily from the photo-oxidation process that condensed semi- or non-volatile compounds and polymerizes organic species in the atmosphere. EC mainly originate from incomplete combustion of biomass and fossil fuels, and have an instantaneous consequence on radiative forcing effect on regional climate. This study was carried out in Dhulikhel Municipality to determine the potential sources and seasonal pathways of carbonaceous aerosols (OC and EC) transporting to receptor site by measurement and modeling approaches. The 72 samples were collected (24-hrs) over a year (January-December 2018) using a medium volume air sampler. The minimum and maximum concentrations of Total Suspended Particulate ranged from 38.00 μg/m^3 to 442.45 μg/m^3. The annual average OC/EC ratio 2.73 ±0.84 indicates the presence of Secondary Organic Aerosols and other major sources of carbonaceous aerosols including biomass burning, vehicular emission, and coal combustion. Hybrid-Single-Particle Lagrangian Integrated Trajectory (HYSPLIT) air-mass back trajectory analysis integrated with meteorological fields was used to identify the potential sources and their atmospheric transport pathway. The back trajectories of the 96-hrs period were plotted at 6-hrs intervals starting from a single observation location at Dhulikhel. The back trajectories were clustered into four distinct seasons to trace temporal variation in the atmospheric aerosols during the study period. The results from the HYSPLIT revealed that the sources of particulate pollutants reaching Dhulikhel are local as well as of regional origin and are mostly transported from the Middle East and South Asian countries like India, Pakistan, Bangladesh, Iran, Saudi Arabia, and Egypt.

Keywords: *Back trajectory, EC, OC, sources, TSP*

Introduction

The atmospheric aerosols consist of a bulky but highly variable mass of carbonaceous aerosols, mostly comprised of Organic Carbon (OC) and Elemental Carbon (EC), constituting nearly 30-70% of the fine particulate mass typically in the urban atmosphere (Cao et al., 2003; Fuzzi et al., 2006; Rengarajan et al., 2007). Generally, OC accounts for 10-50%, while EC accounts for minor portion (<10%) of the total mass concentration of atmospheric particulate matter (Pandit & Seinfeld, 2006).

EC is primary pollutant originates from incomplete combustion of biomass and fossils fuel (Seinfeld and Pandis 1998), while OC is either emitted directly into the atmosphere or formed secondarily from the photo-oxidation process that condensed semi- or non-volatile compounds and polymerizes organic species in the atmosphere (Shakya et al., 2010; Jimenez et al., 2009). During the thermal analysis, EC is differentiated from OC based on thermal or optical measurements, therefore OC can be regarded as the carbon fraction that evolves under a heating cycle in an inert atmosphere, and EC as the fraction that evolves during a subsequent heating process in presence of oxygen (Karanasiou et al., 2015).

Both OC and EC have significant roles in radiative forcing and cloud microphysics, and consequently, in regional climate change and precipitation (Wan

et al., 2017). Also, the relationship between OC and EC provides information on the source of origin of the carbonaceous aerosols and the positive correlation between them indicates a common source of origin (Shakya et al., 2010). The OC/EC ratio is developed as an essential diagnostic index that has been used to reflect the types and source strength of carbonaceous aerosols (Turpin & Lim, 2001). OC/EC ratios depends on emission sources and the secondary organic aerosol formation and the relative amount of OC and EC in the atmosphere, and OC/EC ratios are the important parameters for the assessment of direct/indirect impacts of aerosols on the regional scale radiative forcing (Novakov et al., 2005). However, these ratios depend on the fuel type, quantity, and, more importantly, their combustion efficiency (Bond et al., 2007; Streets et al., 2004).

The particulate matter including OC and EC can remain airborne from days to weeks; therefore, can undergo long-distance transport, producing global and regional in addition to local impacts on the air quality. The transport of air pollutants is mostly driven by weather phenomena like vertical air motions, along with prevailing winds both dilute and disperse particles and gases emitted from various sources (Sen et al., 2017), it is also influenced by seasonal climate and the atmospheric circulation systems (Tripathee et al., 2017). The air-mass back trajectories are valuable for the apportionment of potential source regions and their pathways, and to sightsee the influence of the long-range transport of aerosols (Tripathee et al., 2017).

This study aims to determine the concentrations, seasonality, possible sources, and transport pathways of carbonaceous particles (OC and EC) reaching the receptor site (Dhulikhel, Kavrepalanchok from the aerosol sample collected from January to December 2018. Four distinct seasons—winter (December–February), pre-monsoon (March-May), monsoon (June–September), and post-monsoon (October–November) – are characterized by South Asian Monsoon circulations that affect the weather in Nepal (Bonasoni et al., 2010). Based on this, seasonal variation has been observed in this study.

Materials and Methods

Study site description

Dhulikhel (27.601°North, 85.538°East) is a pleasant hilly city located in the lesser Himalayan zone of central Nepal. The city is situated about 30-kilometer south-east downwind of Kathmandu Valley and about 3 kilometer north-west of Banepa Municipality. The ambient air quality of the study area is influenced by large scale transport of pollutants from the Indo-Gangetic Plains and by local sources around the highly polluted Kathmandu Valley (Shrestha et al., 2010). The southwesterly and northwesterly are major surface winds in the Kathmandu Valley, which merge into the westerly wind channeled to Banepa Valley (Regmi et al., 2003). The particles concentration gets increased by 10-20 $\mu g/m^3$ at Banepa when the westerly winds are blown, carrying pollutants out of Kathmandu Valley towards Banepa through the south-east Sanga Hill (Aryal et al., 2009). During the night time and early morning, the Kathmandu Valley is filled by a thick cold air pool at low elevations favored by the bowl shaped topography of the high mountains (Regmi et al., 2003). Thus, any transport of pollutants from the Kathmandu Valley to the sampling site at Kathmandu University is expected only during day time (Shrestha et al., 2010).

Moreover, the study site is located south-east downwind of Bhaktapur Industrial Estate, as well as several brick kilns that use low-quality coal from January to April (Sarkar et al., 2016). The study site is closer to the junction of two national highways (Araniko and B.P.), which connect central-hilly districts and Terai region to Kathmandu Valley. Aside from these sources, notable polluters include the pharmaceutical, brewing, plastics, brick, and plywood industries.

The study area records a daily mean temperature of 16.85°C (max: 24.32°C and min: 5.94°C) and a mean relative humidity of 95.91% (max: 100% and min: 71.3%) in 2018 (study period). The annual rainfall of 1360 mm was recorded in 2018, substantial rainfall (1008 mm) was observed in monsoon while mild rainfall (329 mm) in pre-monsoon. The meteorology of Dhulikhel and its

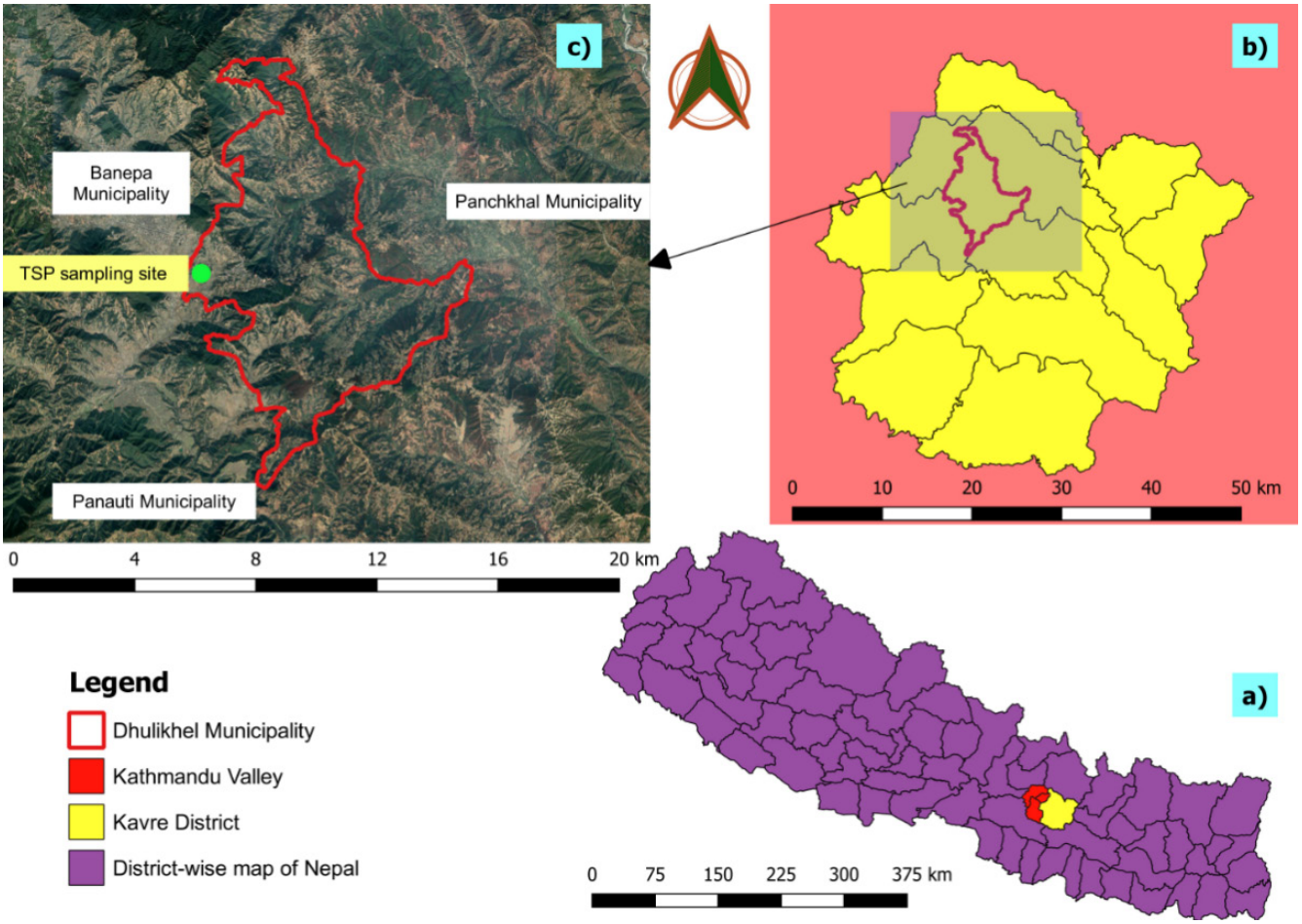

Figure 1: (a) Map of Nepal showing Kathmandu Valley and Kavrepalanchok District (b) Political boundary of Kavrepalanchok district and Dhulikhel Municipality (c) Location of sampling site in Dhulikhel

surrounding regions is controlled by the South Asian Monsoon circulations in the wet season (June-September), while Westerlies dominate the atmospheric circulation patterns in the dry seasons with limited precipitation (Pudasainee et al., 2006; Mues et al., 2017). Moreover, meteorology also gets influenced by local mountain valley circulation (Mues et al., 2018).

Sample collection and analysis

The sampling was carried out under the research framework called Atmospheric Pollution and Cryospheric Change (APCC), which was established in order to examine the transport and influence of atmospheric pollution to cryospheric environment (Kang et al., 2019). Total Suspended Particulate (TSP) samples were collected using medium volume air sampler (T2034, Qingdao Laoying, China) operated at a continuous flow rate of 100 L/min at standard condition based on the local meteorology. The flow rate was calibrated initially during the pre-test. The particles were collected on pre-combusted (550 °C for 5 h) quartz fiber filters (90 mm in diameter, Whatman plc, Maid-stone, UK).

The TSP sampler was set up on the rooftop of three storey building of Kathmandu University Central Library (25.61894° North and 85.53855° East, 1510 meters above sea level), situated approximately 2.5 kilometer north-west of nearest Banepa city in an open space, dominated by residential, agricultural and forest land use.

TSP sample (N=72) was collected on every six days with each sample lasting 24-hours. However, the frequency of sampling was increased for two to three samples per week in pre-monsoon (March-May), slightly modified from Ram et al. (2010b).

Ram et al. (2010a) collected 66 samples, Wan et al. (2017) collected 68 samples, Wan et al. (2019) collected 82 samples for a period of one-year to access carbonaceous aerosols.

The field blank samples were collected approximately once after every five samples at the site. All filters were carefully transferred in a clean disc, wrapped with aluminum foil, and stored in a freezing temperature until further analysis (Tripathee et al., 2016). The aerosol mass loadings were obtained gravimetrically using microbalance by weighing the filters twice before (w_o) and after sampling (w_t). The net accumulation mass for each filter was calculated as the difference between the pre and post sampling weight.

Chemical analysis (OC and EC)

The collected quartz filters were punched in 1.5 cm^2 rectangular filter aliquots to analyze OC and EC using EC–OC analyzer (Sunset Laboratory, Forest Grove, USA) following the thermo-optical transmittance protocol (Ram et al., 2008; Rengarajan et al., 2007). The instrument allocates OC and EC by applying thermal, chemical and optical properties, the OC fraction, evolved during sample heating in the inert atmosphere readily gets converted to CO_2; whereas EC (of refractory nature) is converted to CO_2 under an oxidizing medium, these evolved CO_2 was reduced to methane (CH_4) and measured on Flame Ionization Detectors (FID) (Ram & Sarin, 2010b). For defining the split-point between OC and EC and to correct for the pyrolyzed carbon formed during the initial charring of organic carbon in an inert condition, a 678nm laser source was used and every post-analytical run, fix the volume of methane was injected as an internal standard to assess the performance of FID; whereas potassium hydrogen phthalate was used as an external standard (Ram & Sarin, 2010).

Furthermore, quality assurance was regularly maintained using Standard Reference Materials (GB W08606) designated by National Research Center for Certified Reference Materials, China. Field blank filters were also analyzed similar to test samples.

Cluster analysis of air mass back trajectory

Four-day (96-hrs) air-mass back trajectories arriving at the receptor site (Dhulikhel) were computed using the NOAA–Air Resource Laboratory's Hybrid Single-Particle Lagrangian Integrated Trajectory (HYSPLIT) model (Draxler & Rolph, 2003), at an altitude of 500 m above the ground level, which is within the planetary boundary layer over Himalayas and Tibetan Plateau (Ram et al., 2010a).

The HYSPLIT model was driven by the 3-dimensional meteorological fields adopted from the GADS- 1° dataset available at National Centers for Environmental Prediction Final Analyses-NCEP (3-hours temporal resolution, 1°, 111 kilometer horizontal resolution and 24 vertical levels). The dataset was downloaded from January to December 2018 (ftp://arlftp.arlhq.noaa.gov/pub/archives/gdas1), and these datasets are available in ARL format, readable format for the HYSPLIT model. Total of 1190 trajectories were given as an input to the HYSPLIT model. The four trajectory clusters (1, 2, 3, and 4) were computed for each seasons, as it gives the best representation of air-flow classification (Prabhu & Shridhar, 2019). The HYSPLIT model provides information on the long-range distribution of atmospheric pollutants including carbonaceous aerosols, thus can help to

assume the location of the source of originating air-borne pollutants (Wong, et al., 2012).

Results and Discussions

TSP mass and seasonal variation

The 24-hour average mass concentration of TSP observed to be 226.48 ±106.39 µg/m³ (±Standard deviation), that is quite close to the National Ambient Air Quality Standard (NAAQS), 2012 of Nepal (annual limit: 230 µg/m³). TSP mass ranged from 38.00 µg/m³ (in monsoon) to 442.45 µg/m³ (in pre-monsoon) in 2018. (Table 1).

The mean TSP mass in winter (298.66 ±71.42 µg/m³) and pre-monsoon (277.67 ±90.50 µg/m³) are more than twice that in monsoon (99.02 ±42.52 µg/m³) and post-monsoon (190.86 ±40.38 µg/m³) as presented in Table 1. Moreover, the average TSP mass in winter and pre-monsoon was 31.87% and 22.6% more than the annual average, whereas, in monsoon and post-monsoon, it was 56.28% and 15.73% less than the annual average.

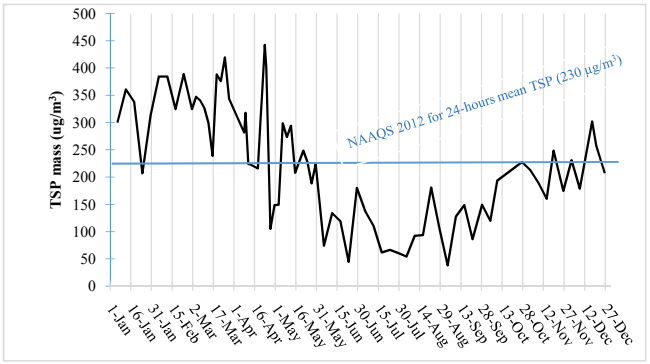

Figure 2: 24-hrs TSP mass collected at sampling site (Jan-Dec 2018)

The study done in Bode, Bhaktapur in April 2013-March 2014 shows that the annual average concentration of TSP was 238.24 ±162.24 µg/m³ and also indicated mass of TSP in ambient air was more in winter (370.21 ±105.12 µg/m³) > pre-monsoon (357.69 ±181.53 µg/m³) > post-monsoon (225.13 ±71.58 µg/m³) > monsoon (113.35 ±51.33 µg/m³) respectively (Tripathee et al., 2017). According to data recorded by the Dhulikhel Air Quality Monitoring Station, established by Department of Environment, the concentration of TSP in 2018 ranged from 511.47 µg/m³ (in winter) to 8.14 (in monsoon) (DOE, 2021).

Sometimes low wind speed and shallow planetary boundary layers in winter and post-monsoon could easily form stagnant weather conditions, which is favorable for the accumulating air pollutants. Meanwhile, excessive rainfall in monsoon lowers TSP levels because it prevents the resuspension of dust and wash-out suspended particulates in the ambient atmosphere. For most dry days, the TSP has exceeded the standard threshold concentration (Table 1).

Source Characterization

Inference from OC and EC concentration and correlation: The annual average OC and EC concentrations in TSP was found to be 18.78 ±12.6 µg/m³ and 6.42 ±2.89 µg/m³, respectively (Table

Table 1: Annual and Seasonal maximum, minimum and average TSP mass at Dhulikhel (2018)(Jan-Dec 2018)

Season	Minimum TSP (µg/m³)	Maximum TSP (µg/m³)	Average TSP (µg/m³)	Number of samples	Number of days TSP exceeded the standard
Pre-monsoon (Mar-May)	74.14	442.45	277.67 ±90.50	30	20
Monsoon (Jun-Sep)	38.00	180.69	99.02 ±42.52	20	0
Post-monsoon (Oct-Nov)	119.73	248.44	190.86 ±40.38	8	1
Winter (Dec-Feb)	178.62	388.76	298.66 ±71.42	14	11
Annual (Jan-Dec)	38.00	442.45	226.48 ±106.39	72	26

2), which accounts for 8.29% and 2.83% of the TSP mass at the study site. The seasonal average mass concentration of EC and OC are presented in Table 2, exhibits lower seasonal variability (except monsoon) suggesting the study site gets common sources and types of aerosols.

The low concentration during monsoon is attributed to relative decrease in the source strength of biomass burning emission and removal by wet deposition (Ram et al., 2010a). The study done by Islam et al., 2022 in January 2018 observed the concentration of OC in $PM_{2.5}$ ranged from 20.7 - 9.6 µg/m^3, and EC in $PM_{2.5}$ ranged from 6.6 - 3.3 µg/m^3 in Dhulikhel.

The OC% and EC% in total carbon (TC) were found to be 72.03 ±5.53% and 27.97 ±5.53%, respectively. The annual and seasonal, maximum, minimum and average OC%, EC% in TC and TC% in TSP mass are presented in Table 2.

The scattered plot (Fig. 3) showed a stronger linear relation (R^2=0.758) between OC and EC in 2018.

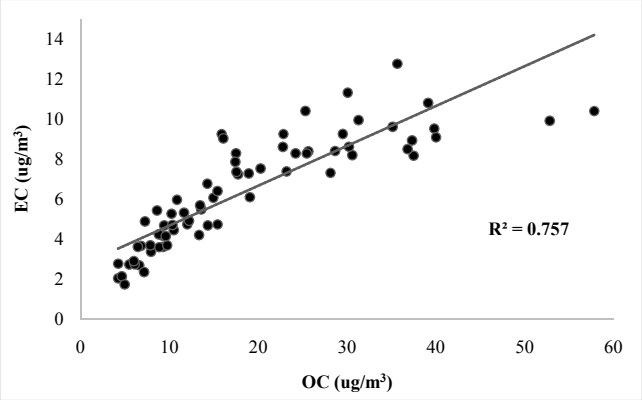

Figure 3: Annual correlation between OC and EC (2018)

The relationship between OC and EC in different seasons are shown in Fig-4. The correlation coefficient of the relationship between OC and EC in pre-monsoon was 0.836, likewise in monsoon, post-monsoon and winter was 0.764, 0.87, and 0.77, respectively (Fig. 4). The significant linear correlation between OC and EC suggests that the carbonaceous aerosols probably have a common source of origin (Ram et al., 2012).

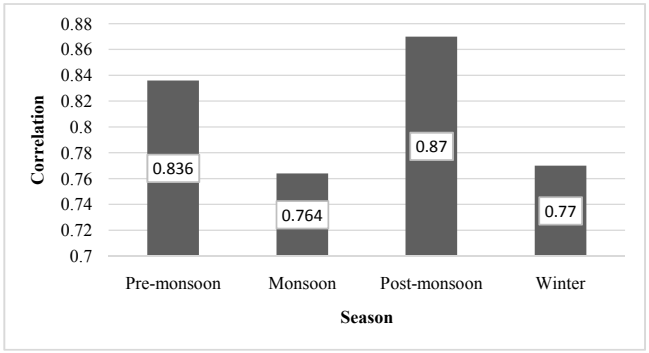

Figure 4: Seasonal correlation between OC and EC (2018)

Inference from OC/EC ratios: The annual average OC/EC ratio was observed to be 2.73 ±0.84 in 2018, the OC/EC ratio in TSP ranged from 1.48 (in monsoon) to 5.55 (in pre-monsoon) as presented in Table 3. The higher OC/EC ratio indicates prevalence of the OC species over EC, attributed to biomass burning, whereas the low ratio indicates the higher emissions from fossil fuel (coal and vehicular exhaust) combustion (Rai et al., 2021). The lower ratio also highlights that the samples contain almost entirely primary carbonaceous compounds which can be influenced by various factors such as meteorology, local sources, and long-range aerosol transport (Dinoi et al. 2017).

Table 2: Average OC%, EC% in total TC and TC% in total TSP mass

Season	Average OC (µg/m^3)	Average EC (µg/m^3)	OC % in TC	EC % in TC	TC % in total TSP mass
Pre-monsoon (Mar-May)	21.62 ±13.67	6.87 ±2.2	73.06 ±6.23	26.94 ±6.23	9.63 ±2.77
Monsoon (Jun-Sep)	7.25 ±2.44	3.22 ±0.91	68.87 ±4.27	31.13 ±4.27	10.84 ±5.97
Post-monsoon (Oct-Nov)	20.19 ±8.13	7.69 ±2.29	71.56 ±4.05	28.44 ±4.05	14.56 ±3.91
Winter (Dec-Feb)	28.39 ±9.07	9.32 ±2.14	74.61 ±4.43	25.39 ±4.43	13.36 ±5.65
Annual	18.78 ±12.6	6.42 ±2.89	72.03 ±5.53	27.97 ±5.53	11.20 ±4.84

The average OC/EC ratio in winter (~3.01) was higher compared to other seasons. Moreover, the average OC/EC ratios in the four seasons (~2.24–3.01) exceeds 2, which indicates the presence of secondary organic aerosol (Chow et al., 2005).

The prior study done in Dhulikhel (January 2018) measured OC/EC ratio in $PM_{2.5,}$ ranged from 2.9 to 3.4, with an average OC/EC ratios of 3.1 (Islam et al., 2022). OC/EC ratios of 2-4 have been previously observed at urban locations in South Asian region (Islam et al., 2020; Sharma et al., 2017; Stone et al., 2010) and are attributed to diesel emissions with OC to EC ratio of 0.6438 (Schauer et al., 1999) and low-efficiency biofuel combustion (Venkataraman et al., 2005).

The literature suggests that the OC/EC ratio can significantly vary while measuring when it is carried away from the source of origin (Lim et al., 2003). As well, it is claimed that the ratios are likely to be influenced by the primary sources of OC, emission sources, SOA formation, and deposition removal rate (Cachier et al., 1996; Ram et al., 2012).

Table 4 depicts the OC/EC ratio of the present study to that of prior studies.

Air-mass back trajectory analysis and satellite observations

To explore the possible source regions of aerosols, four-day air-mass back trajectories were computed using HYSPLIT model for different seasons as shown in Fig-7. However, due to complex topography of the Himalayan region and the influence of local/regional transport processes related to thermal valley winds, back-trajectory results should be described with caution (Tripathee et al., 2017). Moreover, the transport of air pollutants is mostly driven by weather phenomena like vertical air motions, along with prevailing winds both dilute and disperse particles and gases emitted from respective source (Sen et al., 2017).

Consequently, the results of HYSPLIT model have been discussed together with the satellite-derived information on Aerosol Optical Depth (AOD) and fire hotspots for the study period. AOD was obtained from Modern-Era Retrospective analysis for Research and Applications, Version 2 (MERRA-2) sensor at 550 nm wavelength (50 km resolution), while fire hotspots map was generated from Moderate Resolution Imaging Spectro-radiometer

Table 3: Annual and Seasonal OC/EC ratio of the study period (2018)

Season	Min. OC/EC	Max. OC/EC	Average OC/EC	Std. Deviation
Pre-monsoon	1.59	5.55	2.93	1.04
Monsoon	1.48	3.05	2.24	0.44
Post-monsoon	2.10	3.84	2.74	0.55
Winter	1.71	4.33	3.01	0.64
Annual	1.48	5.55	2.73	0.84

Table 4: Comparison of OC/EC ratios with prior studies

Study Area	Study Period	Mean OC/EC ratio	Source	Reference
Northwestern Colorado	1995	1.1	Motor vehicle	Watson et al., 2001
	1995	2.7	Coal combustion emission	
	1995	2.97	Coal-fired boilers	
Xi'an, China	Sept 2003 to Feb 2004	4.10	Vehicular exhaust	Cao et al., 2005
Kathmandu, Nepal	Dec 2007 to Jan 2008	4.47	Vehicular emission	Shakya et al., 2010
Central California	July-Aug 1990	6.6	Biomass burning	Chow et al., 1996
Helsinki, Finland	March 2006 to Feb 2007	3.3	Secondary Organic Carbon	Saarikoski et al., 2008
		6.6	Biomass combustion	
		0.71	Traffic	
Kanpur, India	Jan 2007 to Mar 2008	7.84 ± 2.4	Biomass burning	Ram and Sarin, 2010
Dhulikhel, Nepal	January-December 2018	2.73 ± 0.84		Present study

(MODIS) sensors onboard on Terra satellites of National Aeronautics and Space Administration (NASA).

The air-mass reaching receptor site has illustrated two distinct pathways, i.e., during the dry period air-mass arrives from Indo Gangetic Plain regions of north-west India and eastern Pakistan, while during monsoon air-mass arrives mostly from the Bay of Bengal (Fig-7), which could be the source regions of polluted air mass to our site. Furthermore, the results of active forest fire and non-forest fire hotspots for the study period showed the occurrence of concentrated fire hotspots during dry periods (winter and pre-monsoon) as presented in Fig-5, which causes an intense haze over this region (Tripathee et al., 2017). The prior studies have also reported intensive haze in Indo Gangetic Plain and Himalayan region during the dry periods (Bonasoni et al., 2008; Ram and Sarin, 2015; Tripathee et al., 2017).

Besides, the monthly-averaged AOD map at wavelength of 550 nm showed the higher aerosol loadings across the Indo Gangetic Plain and surrounding region, mostly during dry months (Fig-6). The high AOD during the dry period is mostly from biomass burning (Ram and Sarin, 2015; Wan et al., 2017) and anthropogenic emissions (Tripathee et al., 2017). In the previous discussions, biomass burning and anthropogenic activities were identified for sources of Carbonaceous Aerosols in TSP of the study area. Further, the seasonal pollution over the region is shown by satellite data during the study period, which could have influenced the carbonaceous species at different periods through long-range transport and deposition over the Himalayan region.

The air-mass back trajectories obtained from the HYSPLIT model for different seasons are described below:

a. **Winter season (December-February):** Most of the air-mass arriving at the receptor site originates from Middle East and West Asian countries. Specifically, cluster-1, accounting for about 23% of all trajectories ends up at the Arabian Sea and travels through the Uttarakhand and Madhyapradesh region of India. Cluster-2 and cluster-4 end up in Egypt contributing 23% and 26% of total trajectories, respectively, and cluster-3 originates from Pakistan (Balochistan) contributing 28% of total trajectories reaching Dhulikhel. The plotted trajectory clusters (1, 2 and 3) show more than 60% of trajectories of air mass enter the receptor site through northern India from the Indo-Gangetic Plain which is regarded as the most polluted region in Asia (Thamban et al., 2017; Prabhu & Shridhar, 2019) that can consequently affect the air quality of the study area. Cluster-1 and cluster-3 represent slow-moving air mass compared to cluster-2 and cluster-3. Figure 5 shows that fire incidents are spatially distributed mostly in western and central lesser Himalayan regions in winter season.

b. **Pre-monsoon season (March-May):** The air mass associated with cluster-1 and cluster-3, accounting for about 68% of all the trajectories could be considered major air masses that end up in Pakistan (Punjab) and central Iran, which may have significant implications for aerosol concentration at the study site. Additionally, air-masses cluster-2 ended up in India (Jharkhand), and cluster-4 ended up in Saudi Arabia, contributing 18% and 14% of all trajectories reaching the receptor site.

More than 80% of air mass appeared from strong westerly wind arriving at the study site and entering through the western region of Nepal, northwest India, and Pakistan, and the climate in the Himalayas is strongly influenced by western disturbances during this season (Bonasoni et al., 2010). Similar results were presented by Tripathee et al. (2017); in the dry season, a significant amount of pollutants appeared at sampling sites in the central Himalayas of Nepal (Jomsom and Dhunche) from the Middle East region entering through western Nepal, northwest polluted Indian cities and Pakistan. Furthermore, during the non-monsoon seasons, the transport pathways of air masses arriving at the central Himalayas of Nepal were similar, and northern India appeared to be the foremost

source region of particle pollutants (Tripathee et al., 2017). As shown in Figure 5, most of the fire hotspots were recorded in pre-monsoon when the annual average concentration of Carbonaceous Aerosols and TSP mass concentrations are also higher. The fire hotspots mostly occurred in Terai region.

c. **Monsoon season (June-September):** Most of the air mass reaching Dhulikhel is highly influenced by the South Asian Monsoon as shown in Fig. 6, where air-mass cluster-1 ends up at the Bay of Bengal contributing to the highest proportion of all the air mass (44%) that went through Bangladesh and entering receptor site from the eastern part of Nepal. The air mass of cluster-3 also seems to be prominent because it accounts for 29% of total trajectories reaching the receptor sites bypassing the northeast region of India. The air masses of cluster-2 and cluster-4 were considered to account for a small portion of all the trajectories that originate from India (Uttar Pradesh) and Myanmar, contributing 13% and 15% of total trajectories respectively.

d. **Post-monsoon season (October-November):** Most of the air mass was found to be originated from the Middle East (76%) as shown by air-masses cluster-1 (39%), cluster-3 (30%) and cluster-4 (7%) respectively that ended up in Saudi Arabia, Egypt (near the Red Sea) and Turkey. The air-mass cluster-2, solitarily end

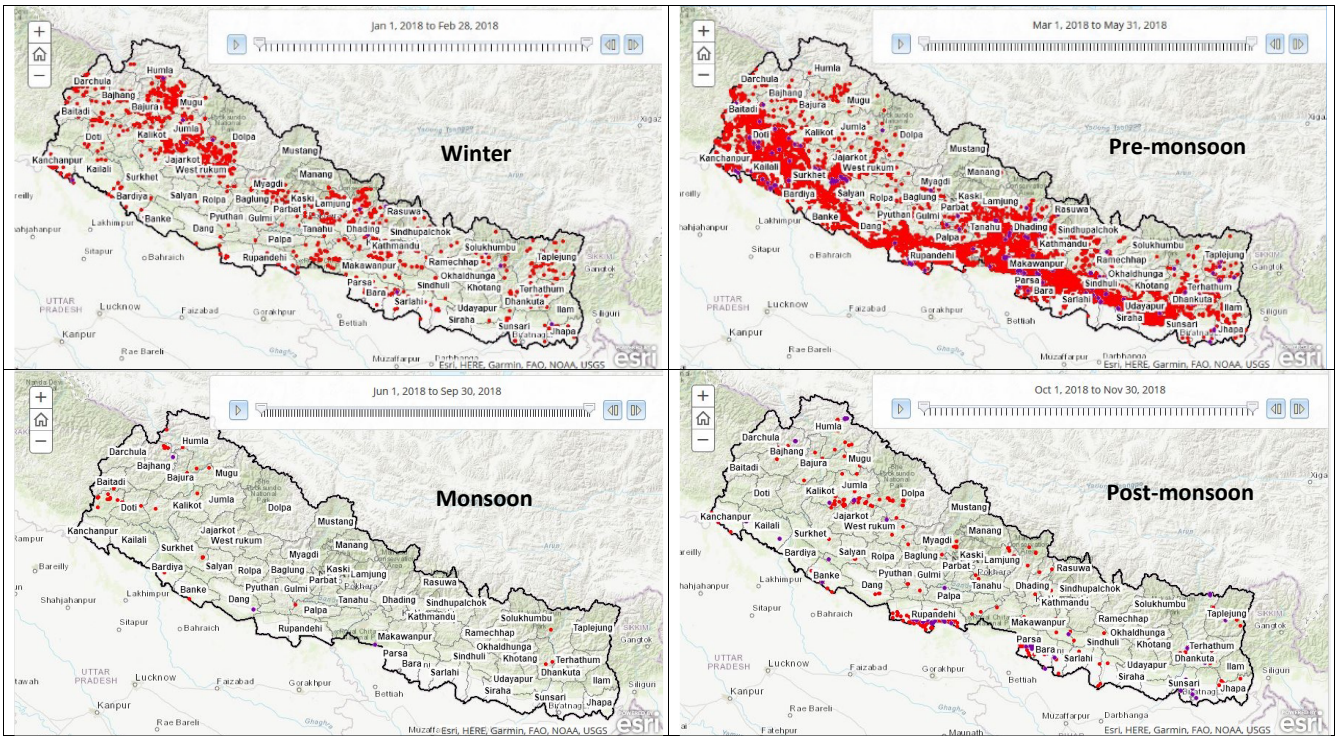

Figure 5: Fire hotspots in four distinct seasons during the study period in 2018 (red dots symbolize the fire hotspots)

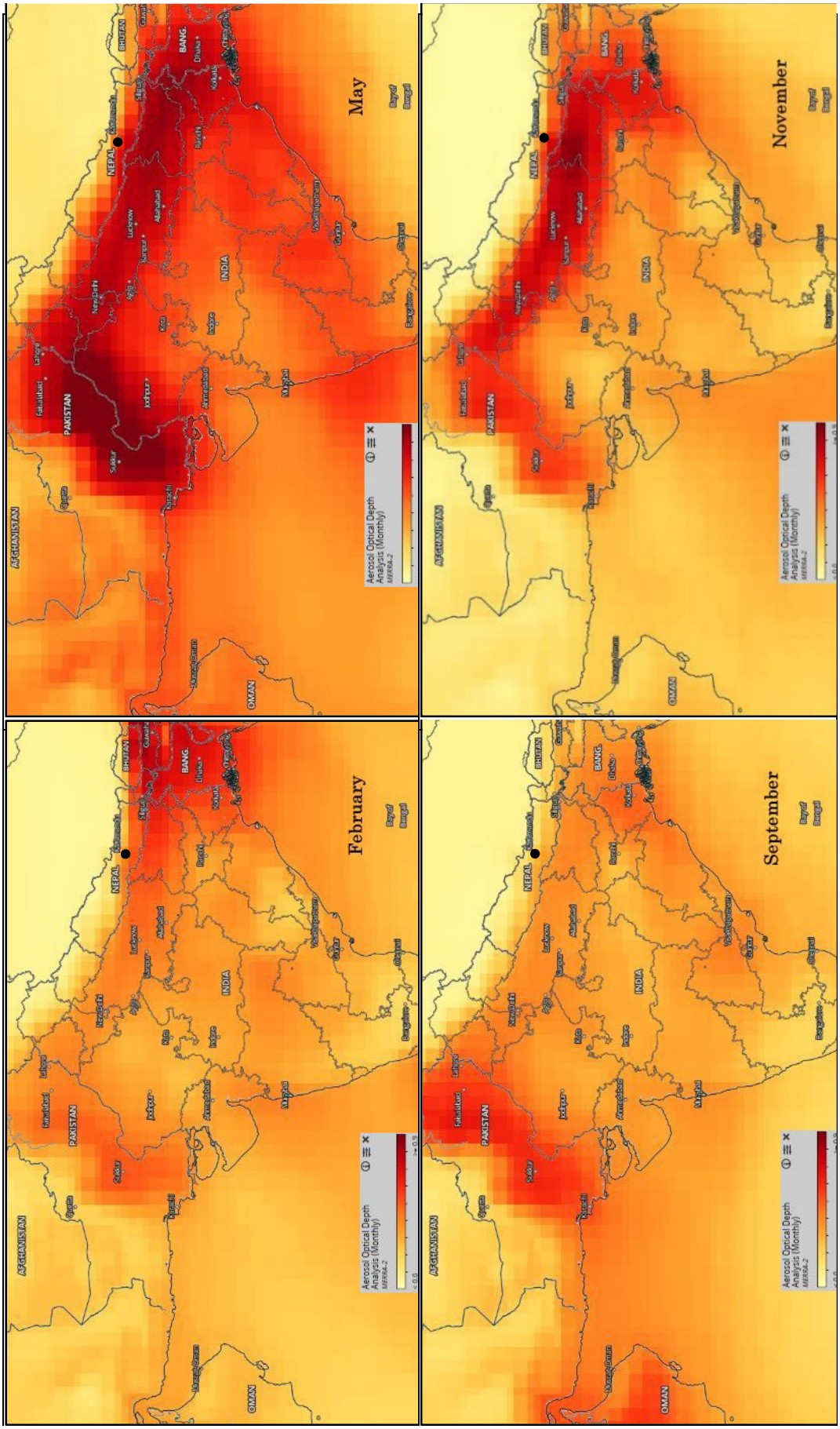

Figure 6: Monthly-averaged AOD map obtained from MERRA-2 sensor (550 nm wavelength; 50 km resolution) in February, May, September and November (2018) The black circle represents the location of the sampling station (Dhulikhel).

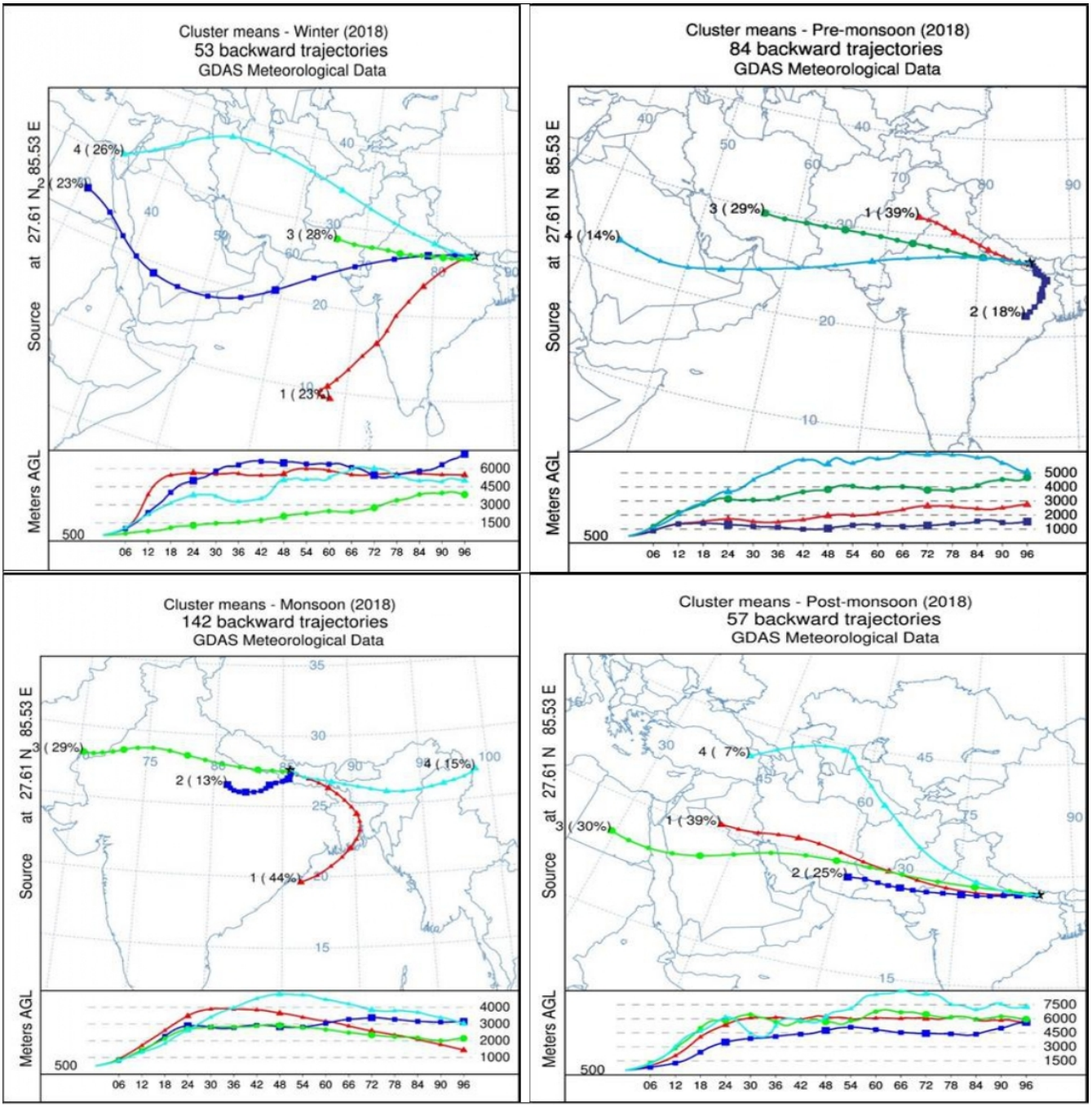

Figure 7: Seasonal air-mass backward transport pathways in Dhulikhel

Conclusion

The measurements of the Carbonaceous aerosols (OC, EC and TC) in the coarse aerosols were conducted during a year between January and December 2018 at the middle hill site of the central Himalayas, Dhulikhel, Nepal. The incidences of surpassing the National Ambient Air Quality Standards, 2012 prescribed limit for a 24-hour daily average mass of TSP were observed with an average mass of 229.35 μg/m^3. The seasonal TSP, OC, and EC levels remained high in pre-monsoon and winter, while during the monsoon, TSP mass is relatively lower due to the settling down of particles from precipitation.

The annual average OC and EC concentrations in TSP was found to be 18.78 ±12.6 μg/m^3 and 6.42 ±2.89 μg/m^3, which accounts for 8.29% and 2.83% of the TSP mass at the study site. Similarly, OC% and EC% in total carbon (TC) were found to be 72.03 ±5.53% and 27.97 ±5.53%, respectively. A

stronger linear relation (R^2=0.758) between OC and EC suggests that the carbonaceous aerosols probably have a common source of origin. The annual average OC/EC ratio was observed to be 2.73 ±0.84 in 2018, the OC/EC ratio in TSP ranged from 1.48 (in monsoon) to 5.55 (in pre-monsoon). The higher OC/EC ratio indicates prevalence of the OC species over EC, attributed to biomass burning, whereas the low ratio indicates the higher emissions from fossil fuel (coal and vehicular exhaust) combustion. Moreover, the average OC/EC ratios in the four seasons (~2.24–3.01) exceeds 2, which indicates the presence of secondary organic aerosol.

The results from air-parcel backward trajectory analysis indicates the atmospheric transportation that appeared to be reaching Dhulikhel is influenced by the two distinct pathways, i.e., from Indo Gangetic Plains (IGP) regions during the dry period (north-west India and eastern Pakistan) and the Bay of Bengal during the monsoon period which could be the source regions of polluted air mass to our site. The air mass appeared to be transported from the Middle East, Bay of Bengal, Arabian Sea, and neighboring South Asian countries, passing over the desert and Indo-Gangetic Plain before reaching Dhulikhel. Thus, the transboundary atmospheric aerosol transport and dispersion were observed to be significant across the western and central regions of Nepal, including the receptor site. Further, the seasonal pollution over the region is shown by satellite data during the study period, which could have influenced the carbonaceous species at different periods through long-range transport and deposition over the Himalayan region.

References

Aryal, R. K., Lee, B. K., Karki, R., Gurung, A., Baral, B., & Byeon, S. H. (2009). Dynamics of $PM_{2.5}$ concentrations in Kathmandu Valley, Nepal. *Journal of Hazardous Materials, 168*(2-3), 732-738.

Bonasoni, P., Laj, P., Marinoni, A., Sprenger, M., Angelini, F., Arduini, J., Bonafe, U., Calzolari, F., Colombo, T., Decesari, S., Di Biagio, C., Di Sarra, A., Evangelisti, F., Duchi, R., Facchini, M., Fuzzi, S., Gobbi, G., Maione, M., Panday, A., Roccato, F., Sellegri, K., Venzac, H., Verza, G., Villani, P., Vuillermoz, E., & Cristofanelli, P. (2010). Atmospheric brown clouds in the Himalayas: first two years of continuous observations at the Nepal Climate Observatory-Pyramid (5079 m). *Atmos. Chem. Phys*., 10, 7515-7531.

Bond, T. C., Bhardwaj, E., Dong, R., Jogani, R., Jung, S., Roden, C., Streets, D. G., and Trautmann, N. M. (2007). Historical emissions of black and organic carbon aerosol from energy-related combustion, 1850-2000. *Global Biogeochemical Cycles*, *21*(2).

Cachier, H., Liousse, C., Pertuisot, M. H., Gaudichet, A., Echalar, F., & Lacaux, J. P. (1996). African fire particulate emission and atmospheric influence, in Biomass Burning and Global Change, edited by J. S. Levine, pp. 428-440, MIT Press, Cambridge, Mass.

Cao, J. J., Lee, S. C., Ho, K. F., Zhang, X. Y., Zou, S. C., Fung, K., Chow, J. C., & Watson, J. G. (2003). Characteristics of carbonaceous aerosol in Pearl River Delta Region, China, during the 2001 winter period. *Atmospheric Environment*, *37*(11), 1451-1460.

Cao, J. J., Chow, J. C., Lee, S. C., Li, Y., Chen, S. W., An, Z. S., Fung, K., Watson, J.G., Zhu, C.S., & Liu, S. X. (2005). Characterization and source apportionment of atmospheric organic and elemental carbon during fall and winter of 2003 in Xian, China. Atmospheric Chemistry and Physics Discussions, *5*(3), 3561-3593.

Chow, J. C., Watson, J. G., Lu, Z., Lowenthal, D. H., Frazier, C. A., Solomon, P. A., Thuillier, R. H., & Magliano, K. (1996). Descriptive analysis of PM2.5 and PM10 at regionally representative locations during SJVAQS/AUSPEX. *Atmospheric Environment*, *30*(12), 2079-2112.

Chow, J.C., Watson, J.G., Louie, P.K.K., Chen, L.W.A., Sin, D. (2005). Comparison of PM2.5 carbon measurement methods in Hong Kong, China. *Environmental Pollution. 137, 334-344.*

Dinoi, A., Cesari, D., Marinoni, A., Bonasoni, P., Riccio, A., Chianese, E., Tirimberio, G., Naccarato, A., Sprovieri, F., Andreoli, V., Moretti, S., Gullì, D., Calidonna, C., Ammoscato, I., & Contini, D. (2017). Inter-comparison of carbon content in PM2.5 and PM10 collected at five measurement sites in Southern Italy. *Atmosphere*, *8*(12), 243.

DOE, 2021. Air quality status of Nepal 2016-2020 - Dhulikhel Air Quality Monitoring Station. Department of Environment (DOE), Ministry of Forest and Environment, Babarmahal, Kathmandu, Nepal.

Draxler, R. R., & Rolph, G. (2003). HYSPLIT (HYbrid single-particle Lagrangian integrated trajectory) model access via NOAA ARL READY website (http://www.arl.noaa.gov/ready/hysplit4.html). *NOAA Air Resources Laboratory*, Silver Spring.

Fuzzi, S., Andreae, M. O., Huebert, B. J., Kulmala, M., Bond, T. C., Boy, M., Doherty, S.J., Guenther, A., Kanakidou, M., Kerminen, V., Lohmann, U., Russell, L.M., & Pöschl, U. (2006). A critical assessment of the current state of scientific knowledge, terminology, and research needs concerning the role of organic aerosols in the atmosphere, climate, and global change. *Atmospheric Chemistry and Physics*, 6(7), 2017-2038.

Islam, Md. R., Jayarathne, T., Simpson, I. J., Werden, B., Maben, J., Gilbert, A., Praveen, P. S., Adhikari, S., Panday, A. K., Rupakheti, M., Blake, D. R., Yokelson, R. J., DeCarlo, P. F., Keene, W. C., & Stone, E. A. (2020). Ambient air quality in the Kathmandu Valley, Nepal, during the pre-monsoon: Concentrations and sources of particulate matter and Trace Gases. *Atmospheric Chemistry and Physics*, *20*(5), 29(27-2951.

Islam, Md. R., Li, T., Mahata, K., Khanal, N., Werden, B., Giordano, M. R., Praveen, P. S., Dhital, N. B., Gurung, A., Panday, A. K., Joshi, I. B., Poudel, S. P., Wang, Y., Saikawa, E., Yokelson, R. J., DeCarlo, P. F., & Stone, E. A. (2021). Wintertime air quality in Lumbini, nepal: Sources of fine particle organic carbon. *ACS Earth and Space Chemistry*, *5*(2), 226-238.

Islam, Md. R., Li, T., Mahata, K., Khanal, N., Werden, B., Giordano, M. R., Praveen Puppala, S., Dhital, N. B., Gurung, A., Saikawa, E., Panday, A. K., Yokelson, R. J., DeCarlo, P. F., & Stone, Elizabeth. A. (2022). Wintertime air quality across the Kathmandu Valley, Nepal: Concentration, composition, and sources of fine and coarse particulate matter. *ACS Earth and Space Chemistry*, *6*(12), 2955-2971.

Jimenez, J. L., Canagaratna, M. R., Donahue, N. M., Prevot, A. S. H., Zhang, Q., Kroll, J. H., DeCarlo, P. F., Allan, J. D., Coe, H., Ng, N. L., Aiken, A. C., Docherty, K. S., Ulbrich, I. M., Grieshop, A. P., Robinson, A. L., Duplissy, J., Smith, J. D., Wilson, K. R., Lanz, V. A., Hueglin, C., Sun, Y. L., Tian, J., Laaksonen, A., Raatikainen, T., Rautiainen, J., Dunlea, E. J., Vaattovaara, P., Ehn, M., Kulmala, M., Tomlinson, J. M., Collins, D. R., Cubisons, M. J., Huffman, J. A., Onasch, T. B., Alfarra, M.R., Williams, P. I., Bower, K., Kondo, Y., Schneider, J., Drewnick, F., Borrmann, S., Weimer, S., Demerjian, K., Salcedo, D., Cottrell, L., Griffin, R., Baltensperger, U., Kolb, C., Middlebrook, A., Wood, E., Williams, L., Trimborn, A., Herndon, S., Jayne, T. J. T., Kimmel, J., Dzepina, K., Zhang, Y., Sun, J., Shimono, A., Hatakeyema, S., Miyoshi, T., Takami, A., & Worsnop, D. R. (2009). Evolution of organic aerosols in the atmosphere. *Science,* 326, 1525-1529.

Kang, S., Zhang, Q., Qian, Y., Ji, Z., Li, C., Cong, Z., Zhang, Y., Guo, J., Du, W., Huang, J., You, Q., Panday, A. K., Rupakheti, M., Chen, D., Gustafsson, Ö., Thiemens, M. H., & Qin, D. (2019). Linking atmospheric pollution to cryospheric change in the third pole region: Current progress and future prospects. *National Science Review*, *6*(4), 796-809.

Karanasiou, A., Minguillón, M. C., Viana, M., Alastuey, A., Putaud, J. P., Maenhaut, W., & Kuhlbusch, T. A. J. (2015). Thermal-optical analysis for the measurement of elemental carbon (EC) and organic carbon (OC) in ambient air a literature review. *Atmospheric Measurement Techniques Discussions, 8*(9), 9649-9712.

Lim, H. J., Turpin, B. J., Russell, L. M., & Bates, T. S. (2003). Organic and Elemental Carbon Measurements during ACE-Asia Suggest a Longer Atmospheric Lifetime for Elemental Carbon, *5 Environ. Sci. Technol., 37,* 3055-3061.

Mues, A., Rupakheti, M., Münkel, C., Lauer, A., Bozem, H., Hoor, P., Butler, T., & Lawrence, M. G. (2017). Investigation of the mixing layer height derived from ceilometer measurements in the Kathmandu Valley and implications for local air quality. *Atmospheric Chemistry and Physics*, *17*(13), 8157-8176.

Mues, A., Lauer, A., Lupascu, A., Rupakheti, M., Kuik, F., & Lawrence, M. G. (2018). WRF and WRF-Chem v3.5.1 simulations of meteorology and black carbon concentrations in the Kathmandu Valley. *Geoscientific Model Development*, *11*(6), 2067-2091.

Novakov, T., Menon, S., Kirchstetter, T. W., Koch, D., &. Hansen, J. E. (2005), Aerosol organic carbon to black carbon ratios: Analysis of published data and implications for climate forcing, *Journal of Geophysical Research*, 110, D21205.

Pandis, S.N., & Seinfeld, J.H. (2006) Atmospheric chemistry and physics: from air pollution to climate change. Wiley, New York.

Prabhu, V., & Shridhar, V. (2019). Investigation of potential sources, transport pathways, and health risks associated with respirable suspended particulate matter in Dehradun city, situated in the foothills of the Himalayas. *Atmospheric Pollution Research*, *10*(1), 187-196.

Pudasainee, D., Sapkota, B., Shrestha, M. L., Kaga, A., Kondo, A., & Inoue, Y. (2006). Ground-level ozone concentrations and its association with NOx and meteorological parameters in Kathmandu valley, Nepal. *Atmospheric Environment*, *40*(40), 8081-8087.

Rai, A., Mukherjee, S., Choudhary, N., Ghosh, A., Chatterjee, A., Mandal, T. K., Sharma, S. K., & Kotnala, R. K. (2021). Seasonal transport pathway and sources of carbonaceous aerosols at an urban site of eastern himalaya. *Aerosol Science and Engineering*, *5*(3), 318-343.

Ram, K., & Sarin, M. M. (2010). Spatio-temporal variability in atmospheric abundances of EC, OC and WSOC over northern India. *Journal of Aerosol Science.,* 41, 88-98.

Ram, K., Sarin, M.M., Hegde, P., 2008. Atmospheric abundances of primary and secondary carbonaceous species at two high-altitude sites in India: sources and temporal variability. *Atmospheric Environment, 42*, 6785-6796.

Ram, K., Sarin,M.M., Tripathi, S.N. (2012). Temporal trends in atmospheric PM2.5, PM10, elemental carbon, organic carbon,water-soluble organic carbon, and optical properties: impact of biomass burning emissions in the Indo-Gangetic Plain. *Environment, Science & Technology, 46*, 686-695.

Ram, K., Sarin, M. M., & Tripathi, S. N. (2010a). A 1-year record of carbonaceous aerosols from an urban site in the Indo-Gangetic Plain: Characterization, sources, and temporal variability. *Journal of Geophysical Research-Atmospheres*, 115(24).

Ram, K., Sarin, M.M, & Tripathi, S. N. (2010b). Inter-comparison of thermal and optical methods for determination of atmospheric black carbon and attenuation coefficient from an urban location in northern India. *Atmospheric Research*, *97*(3), 335-342.

Rengarajan, R., Sarin, M. M., & Sudheer, A. K. (2007). Carbonaceous and inorganic species in atmospheric aerosols during wintertime over urban and high altitude sites in North India, *Journal of Geophysical Research-Atmospheres*, 112, D21307.

Saarikoski, S., H. Timonen, K. Saarnio, M. Aurela, L. Jarvi, P. Keronen, V.-M. Kerminen, and R. Hillamo (2008), Sources of organic carbon in fine particulate matter in northern European urban air, *Atmos. Chem. Phys.*, **8**, 6281-6295.

Sarkar, C., Sinha, V., Kumar, V., Rupakheti, M., Panday, A., Mahata, K. S., Rupakheti, D., Kathayat, B., & Lawrence, M. G. (2016). Overview of VOC emissions and chemistry from PTR-TOF-MS measurements during the SusKat-ABC campaign: high acetaldehyde, isoprene and isocyanic acid in wintertime air of the Kathmandu Valley, *Atmos. Chem. Phys.,* 16, 3979-4003.

Schauer, J. J., Kleeman, M. J., Cass, G. R., & Simoneit, B. R. (1999). Measurement of emissions from air pollution sources. 2. C-1 through C-30 organic compounds from medium duty diesel trucks. *Environmental Science & Technology*, *33*(10), 1578-1587.

Sen, A., Abdelmaksoud, A., Ahammed, Y. N., Alghamdi Mansour φa., Banerjee, T., Bhat, M. A., Chatterjee, A., Choudhuri, A. K., Das, T., Dhir, A., Dhyani, P. P., Gadi, R., Ghosh, S., Kumar, K., Khan, A., Khoder, M., Kuniyal, J. C., Kumar, M., Mahapatra, P. S., Lakhani, A., Naja, M., Pal, D., Pal, S., Rafiq, M., Romshoo, S. A., Rashid, I., Saikai, P., Shenoy, D., Sridhar, V., Verma, N., Vyas, B., Saxena, M., Sharma, A., Sharma, S., & Mandal, T. (2017). Variations in particulate matter over Indo-Gangetic Plains and Indo-Himalayan Range during four field campaigns in winter monsoon and summer monsoon: Role of pollution pathways. *Atmospheric Environment*, *154*, 200-224.

Seinfeld, J.H., & Pandis, S.N. (1998). Atmospheric chemistry and physics. Wiley, New York.

Shakya, K. M., Ziemba, L. D., & Griffin, R. J. (2010). Characteristics and sources of carbonaceous, ionic, and isotopic species of wintertime atmospheric aerosols in Kathmandu valley, Nepal. *Aerosol and Air Quality Research, 10*(3), 219-230.

Sharma, S. K., & Mandal, T. K. (2017). Chemical Composition of Fine Mode Particulate matter (PM 2.5) in an urban area of Delhi, India and its source apportionment. *Urban Climate*, *21*, 106-122.

Shrestha, P., Barros, A., Khlystov, A. (2010). Chemical composition and aerosol size distribution of the middle mountain range in the Nepal Himalayas during the 2009 pre-monsoon season. Atmospheric Chemistry and Physics, 10(23): 11605.

Stone, E., Schauer, J., Quraishi, T. A., & Mahmood, A. (2010). Chemical characterization and source apportionment of fine and coarse particulate matter in Lahore, Pakistan. *Atmospheric Environment*, *44*(8), 1062-1070.

Streets, D. G., Bond, T. C., Lee, T., & Jang, C. (2004). On the future of carbonaceous aerosol emissions, Journal of Geophysical Research-Atmospheres, 109, D24212.

Tripathee, L., Kang, S., Rupakheti, D., Zhang, Q., Huang, J., & Sillanpää, M. (2016). Water-soluble ionic composition of aerosols at urban location in the foothills of Himalaya, Pokhara Valley, Nepal. *Atmosphere*, *7*(8), 102.

Tripathee, L., Kang, S., Rupakheti, D., Cong, Z., Zhang, Q., & Huang, J. (2017). Chemical characteristics of soluble aerosols over the central Himalayas: insights into spatiotemporal variations and sources. *Environmental Science and Pollution Research, 24*(31), 24454-24472.

Tripathi, S. N., Dey, S., Tare, V., & Satheesh, S. K. (2005). Aerosol black carbon radiative forcing at an industrial city in northern India. *Geophys. Res.,* Lett. 32, L08802.

Turpin, B. J., & Lim, H. J. (2001). Species contributions to PM2.5 mass concentrations: Revisiting common assumptions for estimating organic mass. *Aerosol Science and Technology*, *35*(1): 602-610.

Valsaraj, K. T., & Kammalapati, R. R. (2009). Atmospheric Aerosols: Characterization, Chemistry, Modeling and Climate. Washington: *American Chemical Society*.

Venkataraman, C., Habib, G., Eiguren-Fernandez, A., Miguel, A. H., & Friedlander, S. K. (2005). Residential Biofuels in South Asia: Carbonaceous aerosol emissions and climate impacts. *Science*, *307*(5714), 1454-1456.

Wan, X., Kang, S., Li, Q., Rupakheti, D., Zhang, Q., & Guo, J. (2017). Organic molecular tracers in the atmospheric aerosols from Lumbini, Nepal, in the northern Indo-Gangetic Plain/ : influence of biomass burning, 8867-8885.

Wan, X., Kang, S., Rupakheti, M., Zhang, Q., Tripathee, L., Guo, J., Guo, J., Chen, P., Rupakheti, D., Panday, A. K., Lawerence, M. G., Kawamura, K., & Cong, Z. (2019). Molecular characterization of organic aerosols in the Kathmandu Valley, Nepal: Insights into primary and secondary sources. *Atmospheric Chemistry and Physics*, *19*(5), 2725-2747.

Watson, J. G., Chow, J. C., & Houck, J. E. (2001). $PM_{2.5}$ chemical source profiles for vehicle exhaust, vegetative burning, geological material, and coal burning in Northwestern Colorado during 1995. *Chemosphere*, *43*(8), 1141-1151.

Wong, M. S., Nichol, J. E., & Lee, K. H. (2012). Estimation of aerosol sources and aerosol transport pathways using AERONET clustering and backward trajectories: a case study of Hong Kong. *International Journal of Remote Sensing*, *34*(3), 938-955.